Oscillatory activity in cells: multi-stability and hysteresis

J. M. A. M. Kusters[*], J. M. Cortes[*,†], W. P. M. van Meerwijk[**], D. L. Ypey[**], A. P. R. Theuvenet[**] and C. C. A. M. Gielen[*]

[*]*Dept. Biophysics, Radboud University Nijmegen, Geert Grooteplein 21, 6525 EZ Nijmegen, The Netherlands*
[†]*Institute for Adaptive and Neural Computation. School of Informatics, University of Edinburgh, EH1 2QL, UK*
[**]*Dept. Cell Biology, Radboud University Nijmegen, Toernooiveld 1, 6525 ED Nijmegen, The Netherlands*

Abstract. Oscillatory activity of cells has been the topic of many studies. Oscillatory activity can be due to action potential firing corresponding to the well-known Hodgkin-Huxley (HH) type dynamics of ion-channels in the cell membrane or due to IP3-mediated calcium oscillations in the endoplasmic reticulum (ER) causing periodic oscillations of calcium transients in the cytosol. In this study we show that coupling of these two oscillatory mechanisms may reveal a complex, rich spectrum of both stable and unstable states of cells with hysteresis. The predicted bi-stability corresponds to experimentally observed states. This illustrates that the different behavior of cells is not the consequence of differentiation in cells with different properties, but rather reflects different states of a single cell type.

Keywords: calcium oscillator, hysteresis, bistability, Cell signaling
PACS: 05.45.-a ; 05.70.Ln ; 87.16.Ac ; 89.20.-a

Complexity and transitions among stable and unstable states are ubiquitous in biological systems [1, 2]. In physics instabilities playing a role in emerging collective properties have been studied since many years [3, 4, 5, 6]. Recently the phenomenon of multi-stability with hysteresis has also awakened a large interest in biology [7]. Instabilities, for instance, have been shown to be responsible for genetic alterations in tumor development [8, 9] and are also crucial for efficient information processing in the brain, such as in odor encoding [10, 11]. Multistable systems allow changes among different stable states. These transitions can be due to external input and in the absence of external input instabilities may serve as an alternative to switch between different branches of stable states [7]. Bistability is advantageous to prevent the system from reaching intermediate states, such as for example partial mitosis. In addition, hysteresis may help to maintain the system in a particular stable state. Hysteresis locks the cell into a fixed state, preventing it from sliding back to a previous state [12]. This is useful, for instance, in cell mitosis. Once initiated, it should not be terminated before completion [13].

At the network level, multistability, and in particular bistability, plays an important role in cell signaling as well [14, 15]. Communication between cells takes place at synaptic contacts, where an action potential arrival releases a neurotransmitter, thus affecting the post-synaptic potential of the target cell. Typically, each cell receives input from thousands of cells mediated by many different neurotransmitters, and consequently

CP887, *Cooperative Behavior in Neural Systems: Ninth Granada Lectures*
edited by J. Marro, P. L. Garrido, and J. J. Torres

modifying the post-synaptic potential by excitation or inhibition at very different time scales [16]. This information at the cell membrane is transferred to the cell nucleus by so-called second messengers. Calcium is one such second messenger and calcium transients have been observed over a wide range of frequencies, with a chaotic or deterministic pattern [17].

In many systems, intercellular signalling takes place by synchronized oscillatory behavior in networks of electrically coupled cells. This oscillatory behavior is, typically, the result of two different oscillating mechanisms. The first mechanism takes place at the cell membrane and is related to periodic action-potential firing, usually triggered by repeated depolarization of the cell membrane by action potentials arriving from cells elsewhere in the system. Action potentials, arriving at the synapse trigger the release of neurotransmitters, which modulate the conductance of ion-channels in the cell membrane. These changes in conductance modulate the flow of ions through the ion channels, which modifies the membrane potential of the cell. When the membrane potential exceeds a threshold (typically near -40 mV), the cell generates an action potential.

Another mechanism for oscillatory activity is related to oscillations in the concentration of free intracellular calcium by calcium release from the endoplasmic reticulum (ER) store. These intracellular calcium oscillations are due to period oscillations of the so-called IP3- receptor in the ER-membrane. The left panels in Fig. 1 show examples of intracellular calcium oscillations for various IP3-concentrations. These oscillations start at some threshold value for IP3 and continue until at relatively high IP3-concentrations the oscillations stop and the IP3-receptor remains open. This behavior of the IP3-receptor is characterized by two Hopf-bifurcations (see [18]). Related to these calcium oscillations the membrane potential is at rest near - 70 mV, reveals action potential firing, or is constant near -20 mV (right-hand panels in Fig. 1).

In this study we will show how coupling of the plasma membrane oscillator and the intracellular calcium oscillator, which are both relatively simple oscillators, leads to a rich behavior with multiple stable and unstable states with hysteresis. The bi-stability, that follows from the theoretical analyses, corresponds to experimentally observed states. The model, illustrated in Fig. 2, captures the basic characteristics of normal rat kidney (*NRK*) fibroblasts reported in [20] and reproduces, on the basis of single-cell and single-channel data [19], the kinetics for both the membrane ionic currents and the intracellular calcium oscillator.

THEORETICAL MODEL

Dynamics of membrane excitability

The dynamics of the NRK cell membrane excitability is given by a set of equations, which describe the dynamics of the most important ion channels that modulate the conductance of the cell membrane and thereby affect the membrane potential of the cell. Here we will give a short description of the main characteristics of the model. For the full details, see [20].

The rate of change of the membrane potential V_m due to the currents of potassium

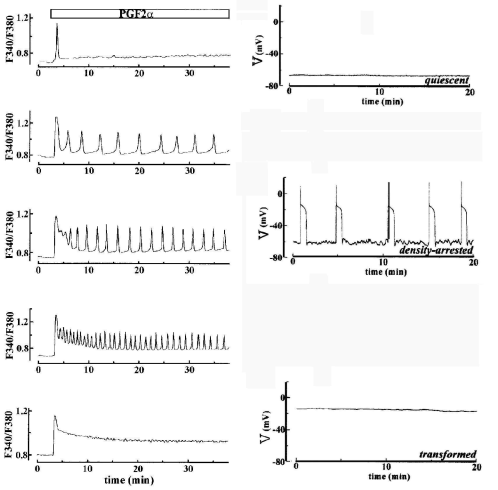

FIGURE 1. Intracellular IP3-mediated calcium oscillations in a NRK-cell (left hand panels) and membrane potentials (right hand side) for various concentrations of IP_3 (increasing from top to bottom). This figure is modified after [19].

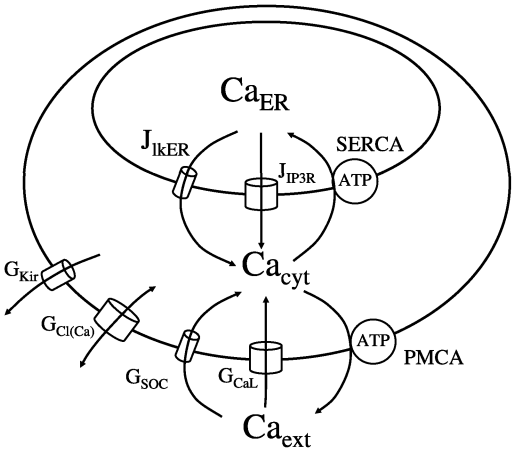

FIGURE 2. Schematic model for *NRK* cells. The membrane excitability consists of inward-rectifying potassium channels (G_{Kir}), calcium-dependent chloride channels ($G_{Cl(Ca)}$), $L-$type $Ca-$channels (G_{CaL}), store-operated channels (G_{SOC}) and a *PMCA* pump. The membrane of the ER contains the *SERCA* pump, the IP_3-receptor (J_{IP_3R}) and leak channels (J_{lkER}).

channels (I_K), L-type Ca-channels (I_{CaL}), calcium-dependent chloride channels ($I_{Cl(Ca)}$),

leak channels (I_{lk}), and SOC-channel (I_{SOC}) is given by

$$C_m \frac{dV_m}{dt} = -(I_K + I_{lk} + I_{CaL} + I_{Cl(Ca)} + I_{SOC}) \tag{1}$$

C_m represents the capacitance of the cell membrane. The equation describing the L-type calcium current (I_{CaL}) as a function of the Hodgkin-Huxley kinetics of the L-type calcium channel, is given by $I_{CaL} = m\,h\,v_{Ca}\,G_{CaL}\,(V_m - E_{CaL})$. This current depends on a Hodgkin-Huxley-type activation variable m, an inactivation variable h, and an inactivation parameter v_{Ca}, which depends on the calcium concentration in the cytosol. The dynamics of the variables m, h and v_{Ca} are described by first-order differential equations of the type

$$\frac{dx}{dt} = \alpha(V)(1-x) - \beta(V)x \tag{2}$$

where α and β are nonlinear functions of the membrane potential V.

The calcium-dependent chloride current $I_{Cl(Ca)}$ is given by

$$I_{Cl(Ca)} = \frac{[Ca^{2+}_{cyt}]}{[Ca^{2+}_{cyt}]+K_{Cl(Ca)}}\, G_{Cl(Ca)}\,(V_m - E_{Cl(Ca)}). \tag{3}$$

The chloride current increases with cytosolic calcium concentration $[Ca^{2+}_{cyt}]$, causing a depolarization to the Nernst potential of chloride ions $E_{Cl(Ca)}$ near -20 mV.

The flux of calcium ions through the cell membrane J_{PM} is the sum of the fluxes of Ca^{2+} ions through the L-type Ca-channel and through the SOC-channel and by extrusion by the PMCA-pump

$$J_{PM} = -\frac{1}{z_{Ca}FA_{PM}}(I_{CaL} + I_{SOC}) - J_{PMCA} \tag{4}$$

Here z_{Ca} represents the valence of the calcium ions, F is the Faraday constant and A_{PM} is the surface area of the membrane. The term $z_{Ca}FA_{PM}$ is necessary to convert the currents (in Ampere) to fluxes of calcium ions.

Finally, calcium in the cytosol is buffered by proteins in the cytosol. The dynamics of buffering is described by first order interactions between $[Ca^{2+}_{cyt}]$ and the concentration of the buffer

$$\frac{d[BCa]}{dt} = k_{on}([T_B] - [BCa])[Ca^{2+}_{cyt}] - k_{off}[BCa] \tag{5}$$

where $[T_B]$ represents the total buffer concentration and $[BCa]$ represents the concentration of buffered calcium.

Dynamics of intracellular calcium oscillator

The dynamics of the intracellular calcium oscillator is described by two differential equations. The dynamics for the calcium concentration in the ER depends on the sum of

fluxes through the IP3-receptor (J_{IP_3R}), leak through the ER-membrane (J_{lkER}) and by removal by the SERCA pump (J_{SERCA}), which results in

$$\frac{d[Ca^{2+}_{ER}]}{dt} = \frac{A_{ER}}{Vol_{ER}}(-J_{IP_3R} - J_{lkER} + J_{SERCA}) \tag{6}$$

where $\frac{A_{ER}}{Vol_{ER}}$ is a conversion factor which transforms the flux of Ca^{2+}-ions through the ER-membrane into changes of Ca^{2+}_{ER}-concentration by the ratio of the size of the surface of the ER-membrane A_{ER} and the volume Vol_{ER} of the ER. The flux through the IP_3-receptor is described by

$$J_{IP_3R} \;=\; f_\infty^3\, w^3\, K_{IP_3R}\,([Ca^{2+}_{ER}] - [Ca^{2+}_{cyt}]) \tag{7}$$

where $[Ca^{2+}_{ER}] - [Ca^{2+}_{cyt}]$ is the concentration difference between calcium in the ER and in the cytosol. K_{IP_3R} is the rate constant per unit area of IP_3-receptor mediated release. f and w represent the fraction of open activation and inactivation gates, respectively, in the IPR_3-receptor. The dynamics of $f(t)$ and $w(t)$ is given by a first order differential equation as in Eq. (2). The time constant for activation is fast relative to the other time constants. Therefore, we will use the steady state value f_∞ in Eq. (7) instead of $f(t)$. f_∞ and w_∞ depend both on the cytosolic calcium concentration and are described by

$$f_\infty = \frac{[Ca^{2+}_{cyt}]}{K_{fIP_3} + [Ca^{2+}_{cyt}]} \tag{8}$$

and

$$w_\infty = \frac{\frac{[IP_3]}{K_{wIP_3}+[IP_3]}}{\frac{[IP_3]}{K_{wIP_3}+[IP_3]} + K_{w(Ca)}[Ca^{2+}_{cyt}]} \tag{9}$$

The membrane oscillator and the IP3-oscillator are coupled by the Ca-concentration in the cytosol (compare Eqs. (7), (8) and (9) with Eqs. (1), (2) and (3)). During an action potential opening of the L-type calcium channel causes a large inward current of Ca-ions in the plasma membrane. The increased $[Ca^{2+}_{cyt}]$ activates the IP_3-receptor by increasing f_∞, Eq. (8), causing an intracellular calcium transient. In the opposite process, IP_3-mediated calcium oscillations cause periodic calcium transients, which open the calcium-dependent chloride channels, Eq. (3). The depolarization of the membrane towards the Nernst potential near -20 mV causes activation of the L-type calcium channels in the plasma membrane. After an action potential or Ca-oscillation the reduction of cytosolic calcium by the activity of the SERCA and PMCA pump reduces $I_{Cl(Ca)}$, such that the membrane becomes subject to the repolarizing to the rest membrane potential near - 70 mV.

Dynamics of the complete cell

The dynamics of the complete single-cell model depends on the time evolution $\frac{d\vec{x}(t)}{dt}$ with $\vec{x}$ the 7-dimensional vector with components $\vec{x}(t) = (m, h, w, [BCa], V_m, [Ca^{2+}_{cyt}], [Ca^{2+}_{ER}])^T$.

Using Eqs. (1), (2), (5) and (6) and keeping in mind the conservation of calcium in the ER, cytosol and outside the cell, this can be written as

$$\dot{\vec{x}}(t) = \vec{f}(\vec{x}(t)) \tag{10}$$

To determine the stability of the complete system $\vec{x}$ we have to find the singular states for the system and then calculate the Floquet multipliers of these singular states.

In order to find the stable states of $\vec{x}(t)$ it is important to notice that the cell with calcium oscillations and action potential firing corresponds to a nonlinear autonomous dynamical system with periodic oscillatory behavior. For a non-oscillating system, stability in a small neighborhood of the singular points is easily found by linearization around the singular points. The eigenvalues of the Jacobian will tell whether a singular point is stable (real part of $\lambda < 0$) or unstable (real part of $\lambda > 0$). In order to find the stable periodic solutions of a periodically oscillating system, we assume that $\tilde{\vec{x}}(t)$ is the periodic solution of the nonlinear dynamical system $\dot{\vec{x}}(t) = \vec{f}(\vec{x}(t))$ ($\vec{x}(t) \in IR^n$). For any perturbation $\vec{y}(t)$ around the stable periodic solution $\tilde{\vec{x}}(t)$ substitution of the solution $\vec{x}(t) = \tilde{\vec{x}}(t) + \vec{y}(t)$ in the differential equation, Taylor expansion around the period solution $\tilde{\vec{x}}(t)$ and retaining only linear terms gives

$$\dot{\vec{y}}(t) = J(\tilde{\vec{x}}(t))\vec{y}(t) \tag{11}$$

where $J(\tilde{\vec{x}}(t))$ is the Jacobian matrix $\nabla_{\vec{x}} f(\tilde{\vec{x}}(t))$ of $f(\vec{x}(t))$. This differential equation for $\vec{y}(t)$ has n linearly independent solutions $\vec{y}_i(t)$, which form the fundamental matrix

$$\Phi(t) = [\vec{y}_1(t), \vec{y}_2(t), ..., \vec{y}_n(t)] \tag{12}$$

It can be shown that any fundamental solution to the matrix of the T-periodic system in Eq. (11) can be written in the form $Y(t) = Z(t)e^{t\Phi}$, where Y, Z and Φ are *nxn* matrices ([21]) with $Z(t) = Z(t+T)$. In particular we can choose $Y(0) = Z(0) = I$, so that $Y(T) = Z(T)e^{T\Phi} = Z(0)e^{T\Phi}$. It then follows that the behavior of the solutions in the neighborhood of $\tilde{\vec{x}}(t)$ is determined by the eigenvalues of the constant matrix $e^{T\Phi}$. The (complex) eigenvalues $\lambda_1, \lambda_2, ..., \lambda_n$ of this matrix are called the Floquet multipliers ([21]). Each Floquet multiplier provides a measure of the local orbital divergence ($|\lambda_i| > 1$) or convergence ($|\lambda_i| < 1$) along a particular direction over one period of the periodic motion. The eigenvalues μ_i of the fundamental solution matrix Φ are called the characteristic exponents of the closed orbit $\tilde{\vec{x}}$.

Note that although the fundamental matrix Φ is not uniquely determined by the solutions of Eq. (11), the eigenvalues of Φ and $e^{T\Phi}$ are. Also notice that the criteria on the Floquet multipliers for convergence (($|\lambda_i| < 1$) correspond to the well-known criteria of $Re(\mu_i) < 0$ for convergence and stability of a simple non-periodic system.

This procedure to find the stable states of a nonlinear periodic oscillator is equivalent to finding the eigenvalues of the monodromy operator (see [22]). The monodromy operator is defined as the linear mapping which maps the initial condition of the system at $t = 0$ into the value of the solution with this initial condition at $T = 2\pi$. For periodic systems the monodromy operator is usually called the Poincare return map or Poincare map. If the eigenvalues μ_i of the (diagonalized) monodromy operator are written as

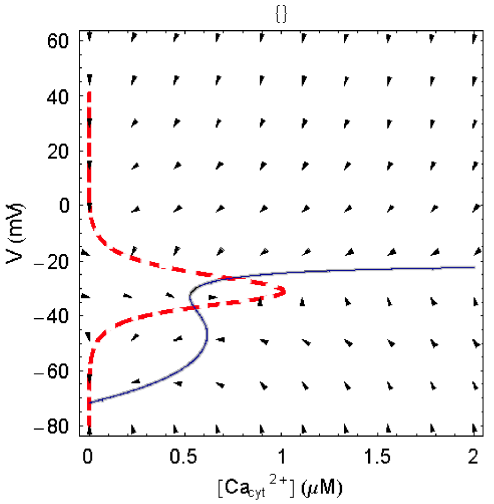

FIGURE 3. (Color online) Nullclines for the isolated excitable membrane. The solid line represents the V-nullcline, whereas the dashed line represents the nullcline for cytosolic calcium concentration. The intersections near (0.01 μM, -70 mV) and (-0.8 μM, -25 mV) correspond to the stable points. The point near (0.55 μM, -40 mV) is a saddle node point.

$\mu_i = e^{2\pi\lambda_i}$, then the nonlinear periodic differential equation can be reduced by means of a linear 2π-periodic substitution $\vec{x}(t) = B(t)\vec{z}(t)$ to the equation with constant coefficients $\dot{\vec{z}} = \Lambda\vec{z}$ where Λ is a diagonal operator with eigenvalues λ_i.

In this study we will explore the bifurcation behavior and local stability of both the electrically excitable membrane and intracellular calcium oscillator, separately, and then compare the results with that for the complete model, where the membrane oscillator and intracellular calcium oscillator are coupled, using the software packages *AUTO* [23] and *XPP* [23].

NUMERICAL SIMULATIONS

Dynamics of the excitable membrane

The dynamics of the cell membrane can be easily studied using the complete model by setting the IP_3 concentration to zero. This eliminates the intracellular calcium oscillations (see Eqs. (7) and (9)). The membrane dynamics are determined by the Eqs. (1) and (2). Fig. 3 shows the null clines for the membrane potential V_m (dashed line) and for the slow variable $[Ca^{2+}_{cyt}]$ (solid line). The two null-clines intersect at the stable points near V_m = -70 mV and $[Ca^{2+}_{cyt}] \approx 0.001\mu M$ and near V_m = -20 mV and $[Ca^{2+}_{cyt}] \approx 0.8\mu M$. The intersection point near (0.55 μM, -40 mV) is a saddle node point. Note that Fig. 3 shows just a 2-dimensional projection of the 7-dimensional state space.

Because changes in the leak of Ca ions through the ER membrane cause variations in

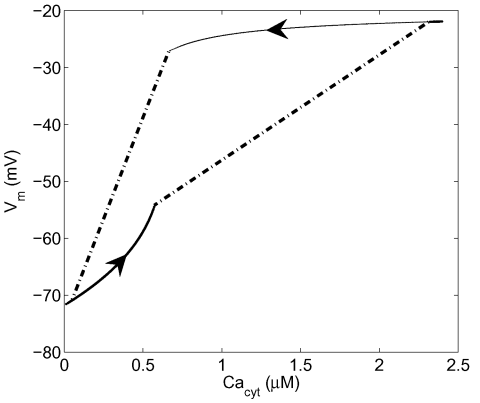

FIGURE 4. The stable states for the electrical membrane. Using K_{lkER} as a control parameter, we represent the stable steady solutions for the calcium concentration in the cytosol (Ca^{2+}_{cyt}) and for the membrane potential (V_m). Solid lines represent stable states. Arrows indicate the direction for increasing and decreasing values of K_{lkER}. Dashed lines represent transitions between stable states.

Ca_{cyt}, the dynamics of the membrane is studied as a function of the leakage parameter K_{lkER}. By changes of the leakage parameter K_{lkER}, the stable points change position. Fig. 4 shows the stable (solid line) and unstable (dashed line) states for the electrical membrane V_m and the calcium concentration in the cytosol (Ca_{cyt} for various values of K_{lkER}. The arrows indicate trajectories for increasing and decreasing values of K_{lkER}. Starting at zero and increasing K_{lkER} (dashed line), the values for the calcium concentration and the membrane potential increase gradually, until $K_{lkER} \approx 53.0 \times 10^{-8} dm/s$. Then, the calcium concentration opens the calcium-dependent chloride channels and the membrane potential depolarizes to the Nernst potential of the $Cl(Ca)$-channels close to $-20\ mV$. As a consequence, $L-$type calcium channels open, causing a calcium inflow from the membrane into the cytosol. This explains the increase of Ca_{cyt} from ≈ 0.6 to $\approx 2.4\ \mu M$. When K_{lkER} is decreased from a high values of $60.0 \times 10^{-8} dm/s$, the $L-$type calcium channels are open, causing an increased Ca_{cyt}. This increased Ca_{cyt} explains why the $Cl(Ca)$-channels are open and thus the membrane potential near -20 mV. If the calcium in the cytosol decreases until a low concentration, the $Cl(Ca)$-channels close and the membrane potential repolarizes to $-70\ mV$. In Fig. 4, all the points in the hysteresis diagram are locally stable around the fixed point solution.

Dynamics of intracellular calcium oscillator

Following a similar plan as in the cell membrane, we illustrate the bifurcation diagram for the calcium concentration in the cytosol as a function of the IP_3 concentration by blocking the $L-$type $Ca-$channels (G_{CaL}=0). For small values of IP_3 there is one single stable steady state. At $IP_3 \approx 0.2\ \mu M$ the dynamics reveals a subcritical Hopf bifurcation,

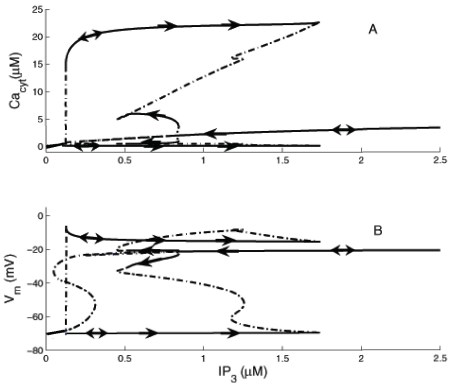

FIGURE 5. The bifurcation diagram for the single-cell model, showing the cytosol calcium concentration (panel *A*) and the membrane potential (panel *B*) as a function of IP_3. Solid and dashed lines correspond to stable and unstable states, respectively. The small arrows on the curves show the direction of evolution of the system for increasing and decreasing values of IP_3. Experimental evidence on the decreasing direction (from left to right) was reported in [24]. Details about the parameters for this model can be found in [20]. The arrow indicates the size of the IP_3-range for hysteresis.

and the system becomes a calcium oscillator in the range. For high IP_3 concentrations ($IP_3 \geq 3.4\ \mu M$) the system meets a subcritical Hopf bifurcation and remains stable at Ca-concentrations near 5 μM.

Dynamics of the complete cell

The bifurcation diagram for the complete single-cell model is illustrated in Fig. 5. As a function of IP_3 we show the cytosolic calcium concentration (panel *A*) and the membrane potential (panel *B*). The solid and dashed lines represent stable and unstable states, respectively. For small IP_3 values in the range $(0.00, 0.15)\ \mu M$, the cell is in the resting condition with a single stable steady state. For $IP_3 > 0.15\ \mu M$ the stable fixed point becomes unstable in a subcritical Hopf bifurcation. Calcium oscillations with action potentials (panel *B*) occur for $IP_3 \in (0.15, 1.75)\ \mu M$. In this regime, a rapid calcium inflow from the ER into the cytosol opens the $Ca-$dependent $Cl-$channel, causing an inward current towards the $Cl-$Nernst potential close to $-20\ mV$, thus leading to depolarization. After closure of the IP_3-receptor, calcium is removed from the cytosol by the Ca-pumps in the cell membrane and ER, leading to repolarization to -70 mV. For $IP_3 > 1.75\ \mu M$, the fixed point $(Ca_{cyt}, V_m) \approx (3.00\ \mu M, -20\ mV)$ becomes stable in a subcritical Hopf bifurcation. Because IP_3 is high, the IP_3-receptor acts as a constant leak of calcium into the cytosol which opens the calcium dependent chloride channels, causing a depolarization to the Cl-Nernst potential near $-20\ mV$ (panel B).

If IP_3 decreases from this point, the cell reveals a complex hysteresis pattern. For decreasing IP_3 concentrations, the system stays in a single stable steady state (solid

line) until $IP_3 \approx 0.85\ \mu M$ with an elevated Ca_{cyt} near $3\ \mu M$ and a membrane potential near $-20\ mV$. Then, crossing through a Hopf bifurcation causes instability (dashed line) forcing the system to behave as a stable oscillator with calcium oscillations with an amplitude of about 6 μM and small membrane potential oscillations around $-20\ mV$. At $IP_3 \approx 0.45\ \mu M$ the stable oscillator with small amplitude becomes unstable (dashed line), returning the system to the stable oscillation with large amplitude (around $20\ \mu M$) and with action potentials in the range $(-70, -10)\ mV$. Finally, for IP_3 values smaller than $0.15\ \mu M$ the system coalesces to a single stable state.

Summary and Conclusions

Summarizing, we present an integrated model reproducing experimental data on calcium oscillations and action potential generation. A bifurcation analysis reveals hysteresis and a complex spectrum of stable and instable states, which allows the system to switch among different stable branches.

ACKNOWLEDGMENTS

We acknowledge financial support from the Nederlandse Organisatie voor Wetenschappelijk Onderzoek (NWO), Ministerio de Educacion y Ciencia (MEC), Junta de Andalucia (JA) and Engineering and Physical Sciences Research Council (EPSRC), projects NWO 805.47.066, MEC FIS2005-00791, JA FQM-165 and EPSRC EP/C0 10841/1.

REFERENCES

1. J. Murray, *Mathematical Biology I. An Introducion*, Springer, 2002.
2. H. Kitano, editor, *Foundations of Systems Biology*, MIT, 2001.
3. H. Haken, *Rev. Mod. Phys.* **47**, 67–121 (1975).
4. B. Jones, *Rev. Mod. Phys.* **48**, 107–149 (1976).
5. C. Normand, Y. Pomeau, and M. Velarde, *Rev. Mod. Phys.* **49**, 581–624 (1977).
6. M. C. Cross, and P. C. Hohenberg, *Rev. Mod. Phys.* **65**, 851–1112 (1993).
7. P. Ashwin, and M. Timme, *Nature* **436**, 36–37 (2005).
8. C. Lengauer, K. Kinzler, and B. Vogelstein, *Nature* **17**, 643–649 (1998).
9. R. Gryfe, H. Kim, E. Hsieh, M. Aronson, E. Holowaty, S. Bull, M. Redston, and S. Gallinger, *N. Engl. J. Med.* **342**, 69–77 (2000).
10. M. Rabinovich, A. Volkovskii, P. L. P, R. Huerta, H. Abarbanel, and G. Laurent, *Phys. Rev. Lett.* **87**, 068102 (2001).
11. G. Laurent, M. S. R. Friedrich, M. Rabinovich, A. Volkovskii, and H. Abarbanel, *Annu. Rev. Neurosci.* **24**, 263–297 (2001).
12. M. Solomon, *Proc. Natl. Acad. Sci. USA* **100**, 771–772 (2003).
13. W. Sha, J. Moore, K. Chen, A. Lassaletta, C. Yi, J. Tyson, and J. Sible, *Proc. Natl. Acad. Sci. USA* **100**, 975–980 (2003).
14. M. Laurent, and N. Kellershohn, *Trends. Biochem. Sci.* **24**, 418–422 (1999).
15. D. Angeli, J. Ferrell, and E. Sontag, *Proc. Natl. Acad. Sci. USA* **101**, 1822–1827 (2004).
16. J. Ferrell, *Curr. Opin. Cell. Biol.* **14**, 140–148 (2002).
17. T. Chay, and J. Rinzel, *Biophys. J.* **47**, 357–366 (1985).
18. Y. Li, and J. Rinzel, *J. Theor. Biol.* **166**, 461–473 (2002).

19. E. Harks, J. Torres, L. Cornelisse, D. Ypey, and A. Theuvenet, *J. Cell. Physiol.* **196**, 493–503 (2003).
20. J. M. A. M. Kusters, M. M. Dernison, W. P. M. van Meerwijk, D. L. Ypey, A. P. R. Theuvenet, and C. C. A. M. Gielen, *Biophys. J.* **89**, 3741–3756 (2005).
21. J. Guckenheimer, and P. Holmes, *Nonlinear Oscillations, Dynamical Systems, and Bifurcations of Vector Fields*, vol. 42, Springer Verlag, 1983.
22. V. Arnold, *Geometrical Methods in the Theory of Ordinary Differential Equations*, Springer Verlag, 1988.
23. T. Fairgrieve, and A. Jepson, *SIAM J. Num. Analy.* **28**, 1446–1462 (1991).
24. E. G. A. Harks, P. H. J. Peters, J. L. J. van Dongen, E. J. J. van Zoelen, and A. P. R. Theuvenet, *Am. J. Physiol. Cell. Physiol.* **289**, C130–C137 (2005).